Available online at www.sciencedirect.com
ScienceDirect
Journal of Nuclear Materials 363–365 (2007) 122–126
journal of nuclear materials
www.elsevier.com/locate/jnucmat

Compatibility of ICRF antennas with W-coated limiters for different plasma geometries in ASDEX Upgrade

Vl.V. Bobkov [a,*], F. Braun [a], R. Dux [a], A. Herrmann [a], A. Kallenbach [a], R. Neu [a], J.-M. Noterdaeme [a,b], Th. Pütterich [b], ASDEX Upgrade Team

[a] *MPI für Plasmaphysik, Boltzmannstr.2, D-85748 Garching, Germany*
[b] *Gent University, EESA Department, B-9000 Gent, Belgium*

Abstract

Since 2005/2006 all side limiters of ICRF antennas in ASDEX Upgrade are W-coated. Comparison of two plasma shapes with high and low triangularity δ shows that the high δ shape leads to the appearance of an intensified antenna–plasma interaction and to a significantly stronger W sputtering. In particular, for (0 π/2) antenna phasing W fluxes as high as 3×10^{19} m^{-2} s^{-1} were measured, a factor of 10 higher than W fluxes for dipole phasing while the difference between the phasings for the low δ discharges is small. Considering general evolution of local W fluxes and sputtering yields at the limiters, it takes ≈20 shots after boronization to increase W yields at the antenna limiters by a factor of 100. More than 100 shots pass until the yields at the limiters far from the antennas reach the same values as at the antenna limiters. W influxes and yields between ELMs show a dependence on RF power close to linear. In H-modes W yields can increase during ELMs by more than a factor of three.

PACS: 52.50.G; 52.40.F; 52.40.H

Keywords: ASDEX Upgrade; ICRF; High-*Z* material; Impurity sources

1. Introduction

Wave heating and current drive in ion cyclotron range of frequencies (ICRF) is used successfully in today's experiments and is relevant for the next step devices. In the ongoing studies of the high-Z first wall materials [1–3] it is of great importance to make ICRF antenna operation compatible with neighboring wall structures [4], as RF induced sheaths may lead to significant sputtering and self-sputtering effects [5].

During the recent years, the tungsten (W) coverage of the first wall components in ASDEX Upgrade (AUG) has been increased [6]. With the introduction of W-coated ICRF antenna limiters in 2005, W sources have increased during ICRF H minority heating. AUG operates in a wide range of parameters, one of them being the plasma shape. While the plasma shapes with high triangularity

* Corresponding author. Fax: +49 89 3299 2558.
E-mail address: Volodymyr.Bobkov@ipp.mpg.de (Vl.V. Bobkov).

0022-3115/$ - see front matter © 2007 Elsevier B.V. All rights reserved.
doi:10.1016/j.jnucmat.2007.01.066

are often preferable for better performance, the impurity sources during ICRF operation can be significantly higher. To shed some light on the reasons for this and on the W source near the antennas during ICRF in general, we study L-mode discharges comparable in terms of plasma density and plasma–limiter distances, but with significantly different shapes. The choice of the L-mode discharges is useful because of a better definition and stationarity of edge plasma conditions. In terms of plasma–antenna interaction and W influxes from the antenna limiters in AUG, L-mode discharges specifically with small antenna–separatrix distance can provide information on the worst case compared to ELM-free H-mode operation (usually at larger antenna–separatrix distances) and can indicate the same tendencies as during ELMs in H-mode due to a stronger plasma–wall interaction during ELMs [7]. We describe also the long-term operation experience of ICRF in AUG, in particular shot-to-shot evolution of W influxes after boronization and the power dependence of W influx.

2. ICRF antennas at ASDEX Upgrade and spectroscopic observations of limiters

The ICRF system at AUG has 4 ICRF antennas with two straps each (see below Fig. 2(a)) [8]. As a standard, dipole phasing (0 π) is used. For 30 MHz frequency, antennas 1 and 2 can be switched to (0 −π/2), antennas 3 and 4 to (0 π/2).

During the 2004/2005 experimental campaign, one W-coated antenna side (poloidal) limiter was mounted in AUG on antenna 4 which was monitored spectroscopically. In 2005/2006 all antenna side limiters are W-coated [6] and antennas 3 and 4 are monitored spectroscopically. For 7 individual poloidal positions shown in Fig. 1(a) and 2(a) there are nine lines of sights (LOSs), six looking on antenna 3 and three looking on antenna 4. W and D(H) line intensities are measured and linked directly to the particle fluxes at the points of observation [9]. In addition, W and D(H) fluxes (Γ_W and Γ_D correspondingly) are measured at poloidal guard limiters which are situated in other toroidal sectors with respect to the ICRF antennas. Effective sputtering yields are calculated by dividing Γ_W by Γ_D [9].

3. Experimental results and discussion

3.1. L-mode discharges with significantly different geometries

Two series of L-mode discharges with pure H minority ICRF heating in D, long after boronization were made with feedback-controlled line averaged density of 4.4×10^{19} m^{-3}, two significantly

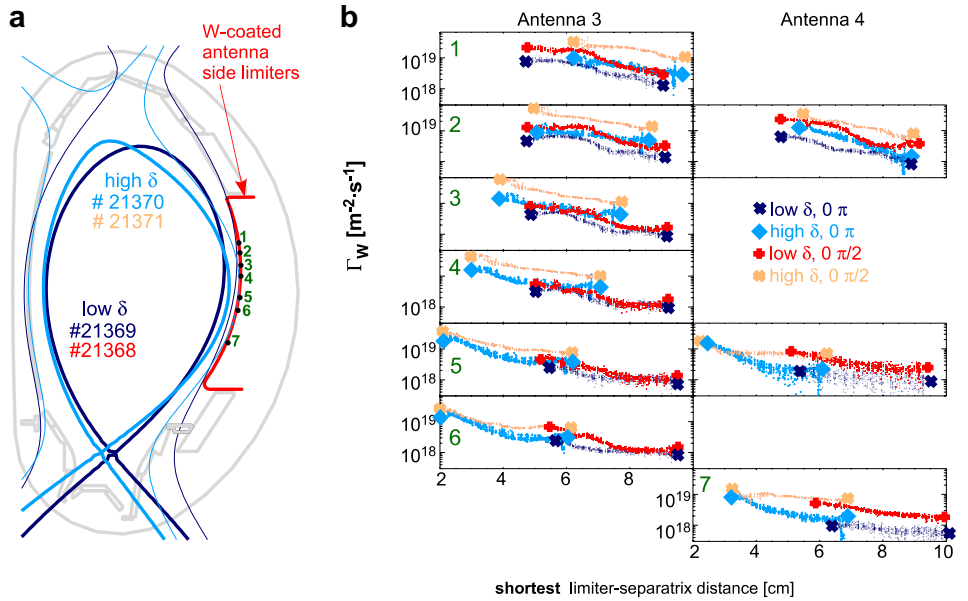

Fig. 1. (a) AUG cross-section with flux surfaces for low and high δ plasma shapes. Thin lines show the surfaces limited by the antenna limiter. Points with numbers locate spectroscopic observations. (b) Spatially resolved W influxes from the antenna limiters for two shapes and two antenna phasings. Large symbols mark the beginning and the end of the data for one discharge.

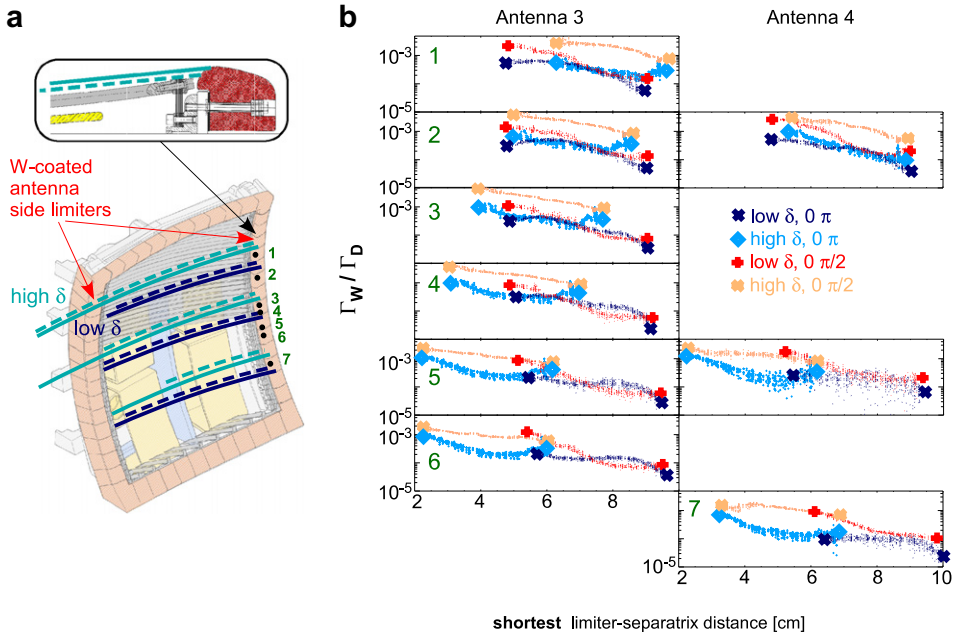

Fig. 2. ICRF antenna with points of spectroscopic observations. Magnetic field lines are sketched for low and high δ plasma shapes: solid lines start on the limiter edge close to plasma, dashed lines start on the limiter in far from plasma. (b) Spatially resolved W yields for two plasma shapes and two antenna phasings.

different plasma shapes (with low plasma triangularity δ: $\delta_{lower} = 0.28$, $\delta_{upper} = -0.06$ and with high δ: $\delta_{lower} = 0.4$, $\delta_{upper} = 0.29$) shown in Fig. 1(a) and radial plasma position scans:

(1) Beginning of 2004/2005, constant ICRF power of 1.6 MW at 36.5 MHz (antennas 3 and 4) with phasing (0 π), 2.5 T, mid plane gas valves.
(2) Middle of 2005/2006, constant ICRF power of 1.6 MW at 30.0 MHz (antennas 3 and 4) with phasings (0 π) and (0 π/2), 2.0 T, divertor gas valves.

We describe briefly the first series (partially discussed in [10]), then dedicate most of this section to discuss the second series of discharges.

Without H puff for both discharges, the H concentration for the high δ case (12%) was twice higher than for the low δ case (6%). With higher neutral fluxes measured at the main chamber, this indicates a much stronger antenna–plasma interaction in the high δ discharge. The interaction is reflected in the significantly higher W influxes from the W-coated antenna limiter measured for high δ for the same antenna–separatrix distances. In particular, LOS (2) looking on the upper part of the limiter measured considerably higher W influxes at high δ. This suggests that the difference of connection lengths of the magnetic field lines starting at observation points for the considered shapes (Fig. 2(a)) might be important: the lines starting from the point of LOS (2) in the high δ shape are not limited by the neighboring structures.

To study if the high δ L-mode discharges tend always to provide conditions for a stronger plasma–antenna interaction, the second series of discharges was conducted. To decrease the possible influence of the gas injection on the interaction, divertor valves were used and the discharges were conducted a long after the last vessel opening.

In contrast to the first series, a higher D puff rate was required for high δ for the feedback control of the central average density. This might be connected to typically different divertor conditions for the high δ where the inner strike point does not fit into the well-baffled region of the divertor. The gas puff rates were lower for (0 π/2) phasing compared to (0 π) indicating the stronger antenna–plasma interaction. The same H concentrations of 5% were measured for both plasma shapes for (0 π) antenna phasing. For (0 π/2) antenna phasing, low δ had 5% of hydrogen whereas high δ had 7%.

The measured W influxes Γ_W from the antenna limiters are presented in Fig. 1(b) as a function of

the shortest limiter–separatrix distance. The figure shows that (a) for (0 π) phasing slightly higher W fluxes are detected at higher δ, for the upper LOSs (1), (2), (3) the differences being larger; (b) for (0 π/2) phasing higher W fluxes are present in comparison with (0 π) and the high δ discharge experiences a significantly larger change of the W fluxes compared to (0 π) than low δ.

(0 π/2) phasing and (0 π)/high δ discharges are characterized by higher values of electron density and temperature measured by Thomson scattering diagnostics between the separatrix and the limiter compared to the (0 π)/low δ. The spectroscopic measurements of H (D) particle fluxes Γ_D characterize local plasma density and allow to estimate effective W sputtering yields Γ_W/Γ_D [9] (Fig. 2(b)). The yields for low and high δ for (0 π) phasing are the same, hence the higher W fluxes observed on the upper LOSs (1), (2), (3) for high δ is due to higher local primary particle fluxes (Fig. 2(a)). For both shapes and (0 π/2) phasing, higher values of W sputtering yield are mainly responsible for the increased W influx. This is not surprising as (0 π/2) phasing is characterized by higher expected RF voltages integrated along the magnetic field lines (voltage compensation by two straps is not as good as for the dipole) and a higher contribution of the power spectrum at $k_{\|} \approx 0$ badly absorbed at the minority resonance (and absorbed parasitically). The (0 π/2)/high δ discharge is characterized by a factor of 10 higher yields for upper LOSs (1), (2), (3) making the combination of (0 π/2) and high δ shape less favorable for operation since the impurity production is strongest.

The lowest gas puffing rates, the highest hydrogen concentration and the highest relative increase of W influxes and yields for high δ, (0 π/2) argue for the sensitivity of the high δ plasma shape with respect to amplification of the antenna–plasma interaction. Other pieces of confirmative experimental evidence are: (a) in contrast to other discharges, there is no short H-mode phase before the radial plasma position scans for (0 π/2)/high δ; (b) going from (0 π) to (0 π/2) phasing low δ shape loses about 27% of stored plasma energy while high δ loses 32%.

Possible explanations for the changes of W yields for high δ shape, consistent with the picture of the poloidal distribution of W influxes are: (1) difference in particle orbits and magnetic field line connection lengths for different δ (Figs. 1(a) and 2(a)); (2) differences in RF voltages integrated over these magnetic lines. On the magnetic field lines bent with respect to the antenna limiter contour for the high δ shape, higher electron temperatures may provide better initial conditions for sputtering and higher local concentration of impurities, the latter being the actual players in W sputtering. These conditions are amplified by high RF induced sheath voltages. First results of calculation of the voltages from antenna modeling by HFSS code [11] agree with the modeled W sputtering yields [9]: in the points of spectroscopic observations the RF voltages are about 100 V.

3.2. Influence of boronization on access and operation of H-mode with ICRF

The experiments reported above were conducted long after boronization (>150 plasma shots), for the same wall conditions. It has been observed before [3,12] that boronization is important for good plasma performance with ICRF and can affect the access to H-mode. In AUG we followed the evolution of W fluxes and sputtering yields over a time period after boronizations on the example of two types of standard low δ discharges repeated once in a while: ICRF only heated and ICRF in combination with neutral beam heating.

Fig. 3 illustrates the evolution of W influxes and yields after boronization. The values are averaged in time and over the poloidally distributed spectroscopic LOSs on the antenna and separately on the guard limiters. Additionally the W densities at the edge of the confined plasma ($T_e \approx 1$ keV) are featured. Data from 'ICRF only heated' discharges

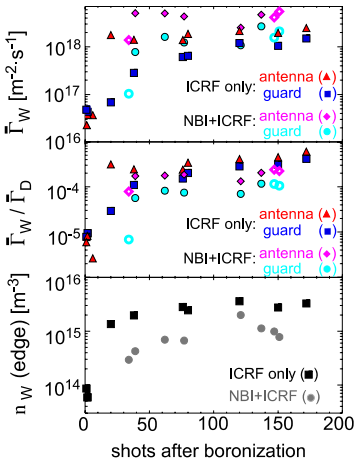

Fig. 3. Shot-to-shot evolution of averaged W influx from the antenna limiters and from guard limiters, W yields and W density at $T_e \approx 1$ keV. Hollow symbols indicate the use of a tangential NI beam.

(1.8 MW, $n_e = 4 \times 10^{19}\,m^{-3}$ if L-mode and $n_e \approx 6 \times 10^{19}\,m^{-3}$ if H-mode) and 'ICRF + NBI heated' discharges (2.5 MW NBI and 2.5 MW ICRF, gas puff feedforward $2.4 \times 10^{21}\,s^{-1}$) discharges following three boronizations are presented in Fig. 3.

W influxes from antenna limiters increase by two orders of magnitude in the first 20 shots after boronization. Then only a very slow increase is observed. These changes are due to the changes of W yields showing the same behaviour. The evolution of the yields is consistent with a gradual removal of boron layers. Boron layers disappear much faster at the antenna limiters than at the guard limiters, i.e boron layers are efficiently removed where high RF fields and high fluxes of primary particles are present. About 70 shots after boronization, the W sources and the W density of the 'ICRF only heated' plasmas increase such that the shots start to experience transition back from H- to L-mode. It is still possible to achieve H-mode with ICRF in this configuration by increasing the power and/or rates of feed forward gas puff. For 'NBI + ICRF heated' discharges, a very similar picture is observed. The W influxes and the yields here are higher, but the edge W densities are lower because of a different penetration of W into the confined plasma.

To illustrate the dependence of W influxes and yields on the RF power, data from an RF power ramp in an H-mode discharge with higher δ, about 50 shots after boronization, are presented in Fig. 4. It shows minimum values of W influxes and yields which align on about a straight line indicating a dependence close to linear [3,12]. Pink symbols show the values during ELMs which represent the values taken in the time when D_α signal from divertor has a deviation larger than 150% of the average D_α level. Since the time resolution of the measurements of W and D(H) fluxes in this case is only 3 ms, the maximum instantaneous values during ELMs can be higher. However we note that the yields during ELMs can be more a factor of three higher than in between ELMs.

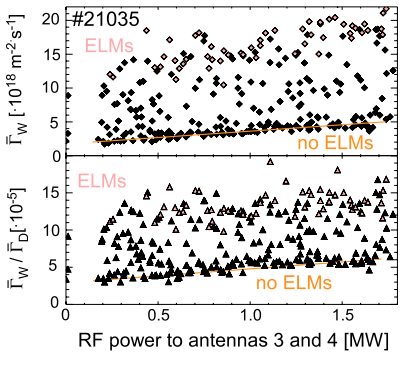

Fig. 4. W fluxes and yields and their variation in H-mode during ICRF power ramp. Pink symbols indicate values during ELMs.

4. Conclusions

High triangularity discharges in ASDEX Upgrade can be characterized by higher W yields and fluxes at W-coated limiters of ICRF antennas during ICRF heating. Antenna–plasma interaction can become much stronger than that in low triangularity plasma shapes, e.g. when using antenna phasing different from dipole. As high triangularity shapes are often preferable for better performance, these have to be used with care together with ICRF.

After boronization, only a limited time is available when W influxes are low. Already some tens of shots after boronization, the W sputtering yields at the limiters and the W densities in the confined plasma have grown considerably such that the access to H-mode with ICRF is affected. The yields at the limiters far from antennas grow much more slowly. During H-modes, W yields and fluxes are generally higher [9], partially due to the presence of ELMs which increase the yields and the fluxes significantly.

To decrease W release during ICRF long after boronization, it is of great importance to study the possible designs of antennas for ASDEX Upgrade with reduced integrated RF voltages along the magnetic field lines and limited contact to W-coated structures.

References

[1] V. Phillips et al., Plasma Phys. Control. Fus. 42 (2000) B293.
[2] A. Kallenbach et al., Nucl. Fusion 47 (2005) B207.
[3] B. Lipschultz et al., Nucl. Fusion 41 (2001) 585.
[4] S. Wukitch et al., Plasma Phys. Control. Fus. 46 (2004) 1479.
[5] J.-M. Noterdaeme, 9th Topical Conference on Radiofrequency Power in Plasmas (Charleston)AIP Conference Proceedings, vol. 244, AIP Press, Melville, NY, 1992, p. 71.
[6] R. Neu et al., J. Nucl. Mater., these Proceedings, doi:10.1016/j.jnucmat.2006.12.021.
[7] T. Eich et al., J. Nucl. Mater. 337 (2005) 669.
[8] J.-M. Noterdaeme et al., Fusion Eng. Des. 24 (1994) 65.
[9] R. Dux et al., J. Nucl. Mater., these Proceedings, doi:10.1016/j.jnucmat.2007.01.014.
[10] Vl.V. Bobkov et al., Nucl. Fusion 46 (2006) S469.
[11] High Frequency Structure Simulator (HFSS), <www.ansoft.com>.
[12] M. May et al., Plasma Phys. Control. Fus. 41 (1999) 45.